

GEOMETRIC RELATIONSHIP OF PREMIXED H₂-AIR FLAME AND WALL IN A TURBULENT CHANNEL FLOW

Ye Wang

Department of Mechanical Engineering
Tokyo Institute of Technology
2-12-1 Ookayama, Meguro-ku,
Tokyo 152-8550 Japan
wang.y.by@m.titech.ac.jp

Sayaka Suzuki

Department of Mechanical Engineering
Tokyo Institute of Technology
2-12-1 Ookayama, Meguro-ku,
Tokyo 152-8550 Japan
suzuki.s.dq@m.titech.ac.jp

Mamoru Tanahashi

Department of Mechanical Engineering
Tokyo Institute of Technology
2-12-1 Ookayama, Meguro-ku,
Tokyo 152-8550 Japan
tanahashi.m.aa@m.titech.ac.jp

ABSTRACT

In this paper, a three-dimensional direct numerical simulation was conducted to investigate the turbulent flame-wall interaction process, considering the premixed H₂-air flame in a turbulent channel flow. The geometric relationship between the near-wall turbulent flame and wall are investigated in a three-dimensional framework by evaluating the near-wall flame's principal curvatures and principal tangent vectors. Then, the impact of the flame-wall geometry on the near-wall flame reaction (near-wall flame quenching) is studied. The result shows that, within the turbulent combustion environment of V-shaped flames in channel flow, the flame's approach to the wall leads to a predominance of three-dimensional characteristics and large curvature wrinkles, manifesting mainly as cylindrical surface features. These cylindrical flame surfaces, under the wall's influence, predominantly align parallel to the wall in proximity to it. As the flame extends from the center of channel to the near-wall area, the previously established positive correlation between the far-wall flame's mean curvature and heat release rate (HRR) diminishes, with a notable decrease in HRR observed on the side of the flame convex to the burned gas. The study also found a more complex correlation between HRR and the flame's principal curvatures, which highlights the critical importance of examining the flame's geometric effects on near-wall thermo-chemical properties through a three-dimensional perspective.

INTRODUCTION

The flame-wall interaction (FWI) is one of the important research topics in turbulent reacting shear boundary layers. Different from the laminar FWI where the flame dynamics and quenching characteristics can be simply treated as a function of flame-wall distance or physical time and combustion conditions, the near-wall turbulence adds additional complexity on the near-wall combustion characteristics by exerting the convection and strain effect on the near-wall flame during local

FWI process. Therefore, from a modeling perspective, exploring the primary influencing factors on near-wall flame dynamics and combustion characteristics is particularly important.

A defining feature of turbulent premixed combustion is the intricate topological structures or wrinkles of the flame as it traverse through turbulent flows. These surface irregularities, induced by turbulence, facilitate a spatial difference in species diffusion and thermal equilibration, and, thus, leading to variances in local heat release rate and flame propagation speed. This property has led many past studies to quantify the degree of wrinkling on flame geometry surfaces (mainly with mean curvature) and discover strong correlations between flame surface curvature and flame dynamics (Chakraborty & Cant (2004); Gashi *et al.* (2005); Chakraborty & Klein (2009)), heat release rates (Echekki & Chen (1996)), and diffusion (Wang *et al.* (2007)). Building upon this, modeling research (Göktolga *et al.* (2021); Xuan *et al.* (2014); Bradley *et al.* (1998)) using flame curvature as a characteristic feature has also been conducted. The research on flame curvature has also expanded into topics such as near-wall combustion and flame-wall interactions in recent years. Zhao *et al.* (2018) investigated the correlation between flow and near-wall flame curvature in a three-dimensional turbulent DNS of near-wall combustion. Zhang *et al.* (2021) studied the impact of flame stretch rate on near-wall fuel consumption rates through direct numerical simulation results of a two-dimensional planar jet flame, finding that the flame normal stretch rate induced by curvature has different effects on near-wall flame and free flame consumption rates. Kosaka *et al.* (2020) measured near-wall flame curvature through experimental studies on methane side-wall quenching. Recently, Kaddar *et al.* (2023) reported a transition in the dependence relationship between flame curvature and heat release rate during the process of flames approaching the wall in direct numerical simulations of lean dimethyl ether/air flames in turbulent channel flow.

Previous research has extensively elucidated the significant influence of flame-wall geometry on the near-wall flame

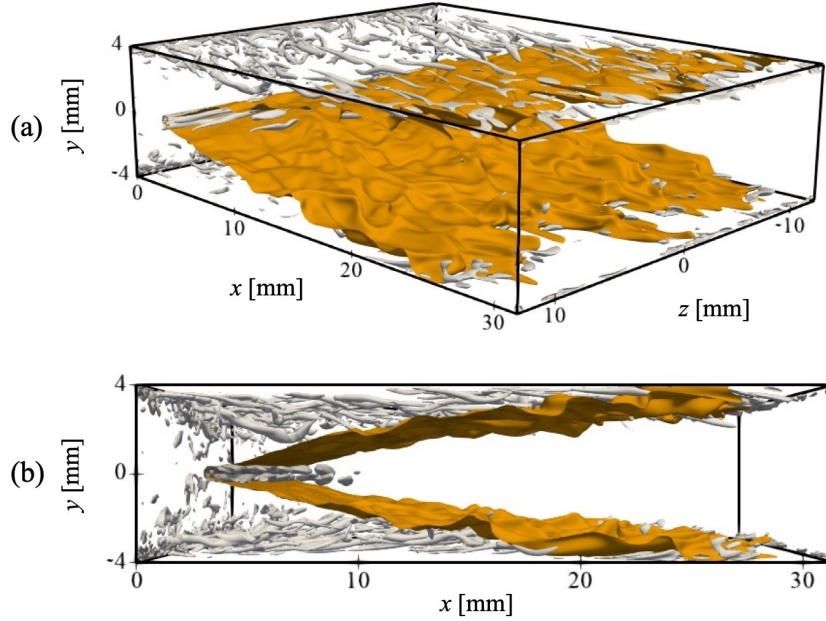


Figure 1. Snapshot of the V-shape H_2 -air flame in the turbulent channel flow (orange: flame surface, white: turbulent vortices). Axial view (a), and side view (b).

reacting features. However, it is worth noting that the previous research, typically focusing on the mean curvature, might not be enough to well describe the inherently three-dimensional features of near-wall turbulent flames. While, to gain a further understanding of the mechanisms governing turbulent FWI, a comprehensive three-dimensional characterization of the geometric attributes of the flame-wall interface is imperative. To achieve that, a three-dimensional direct numerical simulation has been conducted in this study, considering a premixed hydrogen-air V-shape flame in a turbulence channel flow. The principal curvatures and their corresponding tangent vectors of the near-wall flame surface have been investigated with regard to their relationship to the local wall.

NUMERICAL SETUPS

The present DNS is conducted with an in-house code TTX (Tanahashi *et al.* (2000)), where fully compressible conservation equations for mass, momentum, energy, and chemical species mass fractions are considered. A detailed mechanism (Li *et al.* (2004)) with 9 species and 19 reactions is utilized for the H_2 combustion.

The combustion simulation is conducted in a turbulent channel flow. A snapshot of the combustion is shown in Fig. 1. This configuration was previously employed by the DNS of (Gruber *et al.* (2010)), where the flame is anchored by the high-temperature rod in the upstream centre of the channel and gets extended to the upper and lower walls. Meanwhile, a fully developed turbulent channel flow is constructed in the channel so the flame interacts with the wall under the near-wall turbulence's significant effect. In the current simulation, the domain size ($l_x \times l_y \times l_z$) is $8\pi \times 8 \times 10\pi \text{ mm}^3$. The preheat temperature of the H_2 -air mixture is set at 700 K, and the pressure is set at 1.0 atmosphere pressure. The equivalence ratio of the combustion is 1.0. The streamwise boundaries of the domain are respectively set as the inflow and outflow conditions, transverse ones as the periodical boundaries, and vertical ones as the iso-thermal walls with the temperature at 700 K. The tur-

bulent channel flow is simulated by another DNS code named TCF with incompressible N-S equations. It is set as the initial velocity field and implanted as the inflow condition. Its friction Reynolds number, Re_τ , is 180. A pre-test was conducted to simulate this turbulent channel flow with TTX without reaction, and the obtained results were compared with the original non-reacting flow calculated by TCF code. Figures 2-4 plot their mean velocity, profiles shear stress, and turbulent kinetic budget distributions conditioned on wall distance. As can be seen, the statistics of the non-reacting turbulent channel flow shows a good consistency between the original results and the results calculated with compressible combustion code.

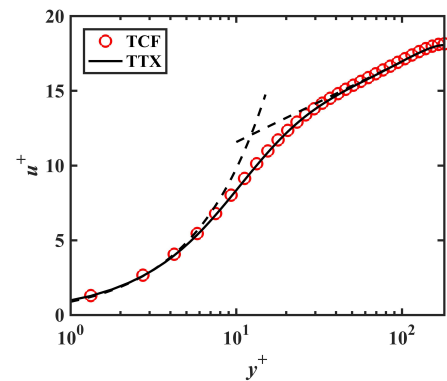


Figure 2. Profiles of the normalized mean velocity of turbulent channel flow calculated by TCF and TTX codes.

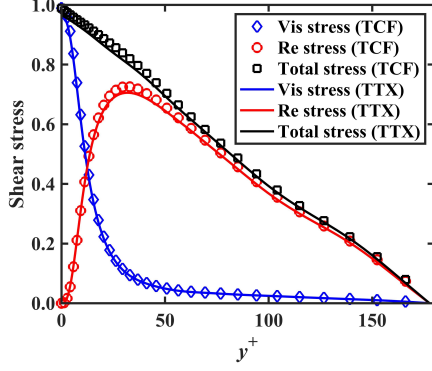


Figure 3. Profiles of the shear stress of turbulent channel flow calculated by TCF and TTX codes.

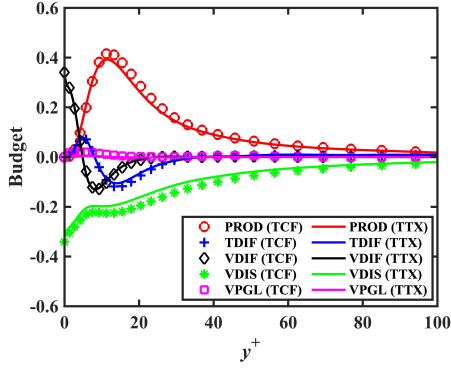


Figure 4. Profiles of the budgets of the turbulent kinetic energy of turbulent channel flow calculated by TCF and TTX codes.

RESULTS AND DISCUSSIONS

Statistical Characteristics of Principal Curvatures of Flame Surface

In the current DNS study, the flame surface is defined as the iso-surface of the progress variable ($c = (Y_{F,u} - Y_F) / (Y_{F,u} - Y_{F,b})$) at $c = 0.7$. Here, Y_F , $Y_{F,u}$, and $Y_{F,b}$ denote the mass fraction of H_2 of local position, unburned gas and burned gas, respectively. The principal curvatures (k_1 and k_2), and their corresponding principal tangent vectors (\mathbf{t}_1 and \mathbf{t}_2) can be determined on that basis, and the flame's three-dimensional topological features and the flame-wall geometric relationships can be evaluated. Here, with the current definition of flame surface, the curvature with an above-zero value indicates that the local flame is convex towards the burned gas. Conversely, the below-zero curvature means the local flame is convex to the unburned gas. Further, if the local flame's principal curvatures satisfy $k_1 > 0$, $k_2 > 0$, and $k_1 \approx k_2$, then it has a spheric shape convex towards the burned gas (S-B); $k_1 > 0$ and $k_2 = 0$ indicating the local flame with a cylindrical shape convex towards the burned gas (C-B); $k_1 > 0$ and $k_2 < 0$ indicating the local flame with a hyperbolic shape (H-B); $k_1 = 0$ and $k_2 < 0$ indicating the local flame with a cylindrical shape

convex towards the unburned gas (C-U); $k_1 < 0$, $k_2 < 0$, and $k_1 \approx k_2$ indicating the local flame with a cylindrical shape convex towards the unburned gas (S-U).

Figure 5 shows the joint probability density function (PDF) of k_1 and k_2 for the flame elements respectively in the three sub-regions of the turbulent channel flow, conditioned by a normalized flame-wall distance (Peclet number, Pe (Poinot *et al.* (1993))) and the wall distance non-dimensionalized by the wall unite (y^+). They are far-wall region ($Pe > 15$, $y^+ > 13.8$), wall-influence region ($5 < Pe < 15$, $4.6 < y^+ < 13.8$) and near-wall quenching region ($Pe < 5$, $y^+ < 4.6$). As can be seen in Fig. 5(a) for the flame with $Pe > 15$ ($y^+ > 13.8$), the highest PDF of the flame's curvatures is located in the region where both k_1 and k_2 are close to zero. The flame elements with a large curvature are mostly concentrated in the S-B, C-B, and H-B regions, indicating that the wrinkled flame in this sub-division is mostly convex to the burned gas. Compared with the flame in the other regions, this part of the flame elements is less affected by the wall, and the flame geometric structures are mostly determined by the flame-turbulence interaction. With the flame in the wall-influence region, in Fig. 5(b), it can be seen that the PDF of the flame increases along the k_1 -increasing and k_2 -decreasing direction. In other words, the PDF of the flame with greater $|k_m|$ increases and the flame becomes more distorted. In addition, the increase of PDF is most prominent in the C-U and C-B regions. Compared with the far-wall region, the turbulent intensity here is greater, and the flame-turbulence interaction in this region is more intensive. As a result, the PDF of the flame with large curvatures increases in all sub-divisions of (k_1 , k_2) diagram. Meanwhile, as the flame gets closer to the wall, the effect of the wall becomes obvious. Due to the cooling effect of the wall, the propagation speed of the flame decreases as the flame gets closer to the wall. The gradient of the propagation speed of the flame surface along the wall-normal direction causes the near-wall flame to show a cylindrical shape with its axis parallel to the wall. That explains why the PDF of the flame with large curvatures increases more in the C-U and C-B regions in Fig. 5(b). As for the flame in the quenching region (Fig. 5(c)), the turbulence goes weak in this region and the effect of the wall on the flame's geometric structure takes dominance. As a result, compared with Figs. 5(a,b), the PDF of the flame with large curvatures only increases in C-U and C-B regions where the flame exhibits a cylindrical shape.

Given that the cylindrical flame takes the majority in the near-wall flame topology, Figure 6 further shows the locative relations between the cylindrical flame and the wall with the flame extending from the center of the channel to the wall. Here, for C-U flame elements, the axis of their cylindrical surface are aligned to their principal tangent vectors \mathbf{t}_1 , and \mathbf{t}_2 for C-B flame elements. Therefore, the locative relations between the C-U, C-B flame and wall can be parameterized by $\cos\gamma_1 = \mathbf{t}_1 \cdot \mathbf{n}_w$ and $\cos\gamma_2 = \mathbf{t}_2 \cdot \mathbf{n}_w$, Here \mathbf{n}_w denotes the wall normal unit vector.

In Fig. 6(a), it can be observed that for the C-U type flame, in the region far from the wall, the flame with ($\cos\gamma_1 > \cos 60^\circ$) account for the majority, meaning that the axes of the cylindrical surfaces are predominantly perpendicular to the wall. As the flame-wall distance decreases, the proportion of C-U flames oriented perpendicular to the wall continues to decrease. Conversely, the proportion of C-U flames tilted and parallel to the wall increases. In the region where y^+ ranges from 10^0 to 10^1 , it can be seen that the proportions of the three positional relationships of C-U flames are maintained at the same level. As the flame-wall distance further

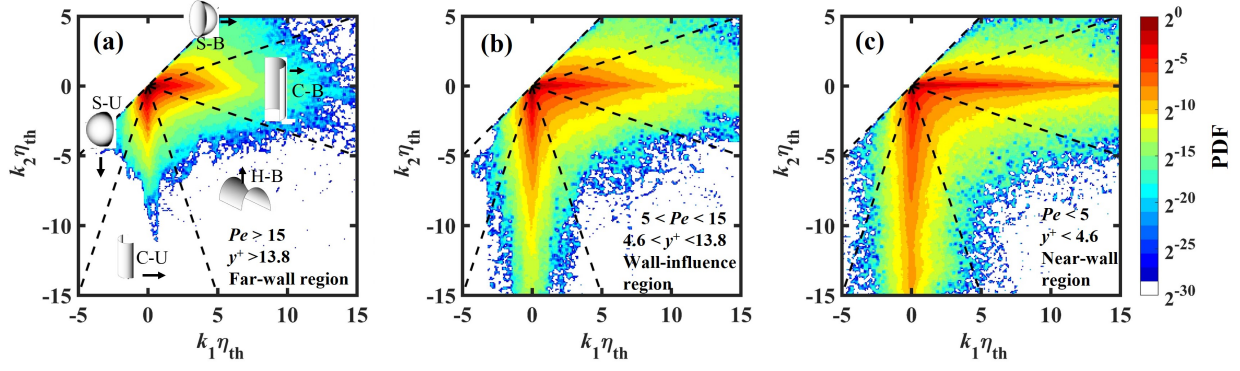


Figure 5. Joint probability density function between flame's principal curvatures (k_1, k_2) in different near-wall turbulent regions

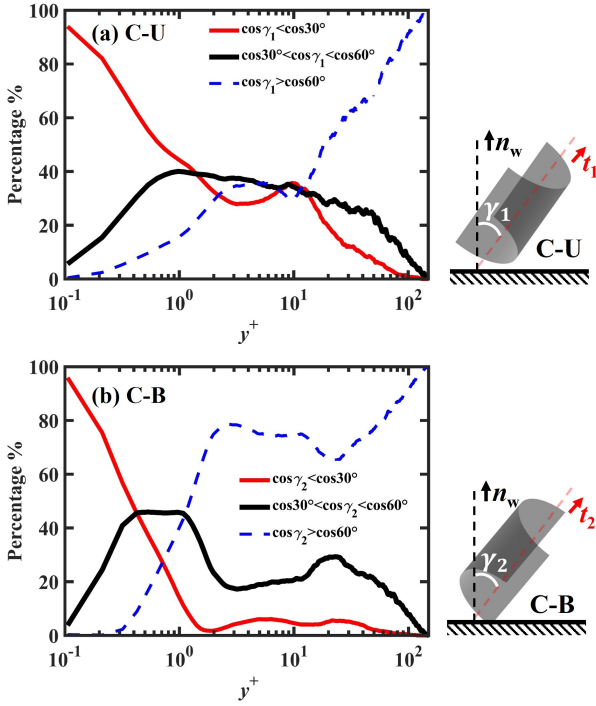


Figure 6. Proportions of C-U and C-B flame elements with $\cos\gamma_1/\cos\gamma_2$ ranges as functions of y^+ .

decreases, the effect of the wall on the positional relationship of flames with respect to the wall becomes more pronounced. The proportion of C-U flames oriented perpendicular to the wall or tilted towards the wall decreases, and C-U flame tends to be distributed parallel to the wall. In Fig. 6(b), the overall trend of the positional relationship between the C-B type flame and the wall as the flame approaches the wall can be observed. The proportion of flames oriented perpendicular to the wall decreases as the flame-wall distance shortens. Near the wall, the majority of flames are oriented parallel to the wall.

Based on the analysis of flame principal curvature and the angle between the principal tangent vector and the wall normal direction, it can be found that in the current turbulent combustion scenario of V-shaped flames in the channel flow, as the flame approaches the wall, the flame surfaces with three-dimensional characteristics and large curvature wrinkles mainly exhibit cylindrical surface features. Furthermore, influenced by the wall, these cylindrical flame surfaces are predominantly parallel to the wall near the wall.

Effect of Flame Topological Structure on Local Heat Release Rate

With the flame surface's topological characteristics are discussed through principal curvature and principal tangent vectors, in this section, the impact of the flame surface's three-dimensional geometric properties on its thermal-chemical reaction intensity is discussed. Figure 7 illustrates the contour of joint probability density distribution of flame mean curvature and local heat release rate (HRR) at different flame-wall distances. Here, mean curvature (k_m) and HRR (ΔH) are dimensionless based on the flame thermal thickness (δ_{th}) and peak heat release rate of the corresponding laminar flame (ΔH_L) under current combustion conditions. In Fig. 7(a), it can be seen that the high values (red lines) of the joint PDF are mainly concentrated at $k_m = 0$ and $\Delta H/H_L = 1.0$. Additionally, there is a clear positive correlation between HRR and mean curvature. This is what has been widely reported in the wall-free turbulent flame research (Tanahashi *et al.* (2000)). In Fig. 7(b), as the flame approaches the near-wall influence region, the positions with larger PDF values correspond to decreasing $\Delta H/H_L$ and are primarily distributed in the region where $\Delta H/H_L < 1.0$. Compared to flames far from the wall, the positive correlation between $\Delta H/H_L$ and k_m becomes less pronounced near the wall, especially at positions with large $|k_m|$ values, where no significant dependency between $\Delta H/H_L$ and k_m can be observed. In Fig. 7(c), when the flame enters the near-wall quenching region, the PDF exhibits a wide distribution in the high $\Delta H/H_L$ region. This may be due to recombination reactions occurring near the wall when the flame quenches, leading to a high level of HRR (Gruber *et al.* (2010)).

To further study the dependency of HRR on curvature, Fig. 8 shows the distribution of $\Delta H/H_L$ conditioned on the principal curvature. It can be observed in Fig. 8(a) that, for the flame is far from the wall, high $\Delta H/H_L$ is distributed in the S-B and C-B regions, and overall, $\Delta H/H_L$ increases in the direction of increasing k_m . Meanwhile, there is no significant variation of $\Delta H/H_L$ along the direction where k_m remains constant. This supports the results in Fig. 7(a) where HRR shows a positive correlation with k_m , without further complexity in the (k_1, k_2) space. While, in Fig. 8(b), as $\Delta H/H_L$ decreases overall, the decrease in $\Delta H/H_L$ is particularly significant in the C-B region, especially in the region where k_2 is close to 0. In comparison, the decrease in $\Delta H/H_L$ in the S-U and C-U regions is not so significant, and the results in Figs. 8(b1-b3) further elaborate on this point. Due to these combined factors, the positive correlation between $\Delta H/H_L$ and k_m no longer exists. On the other hand, $\Delta H/H_L$ exhibits a more complex correspondence with (k_1, k_2) . This complexity is more pronounced in the near-wall quenching region (Fig. 8(c)), where

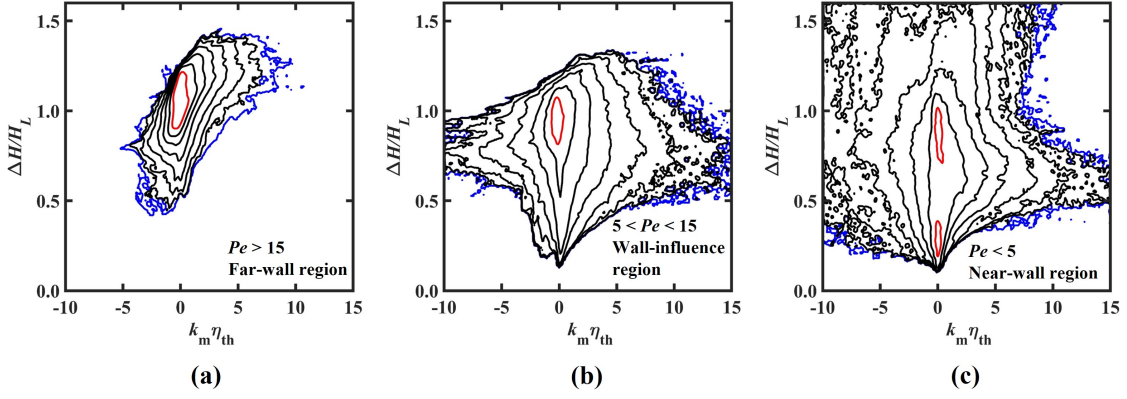


Figure 7. Contours of joint probability density function between flame's mean curvature k_m in different near-wall turbulent regions.

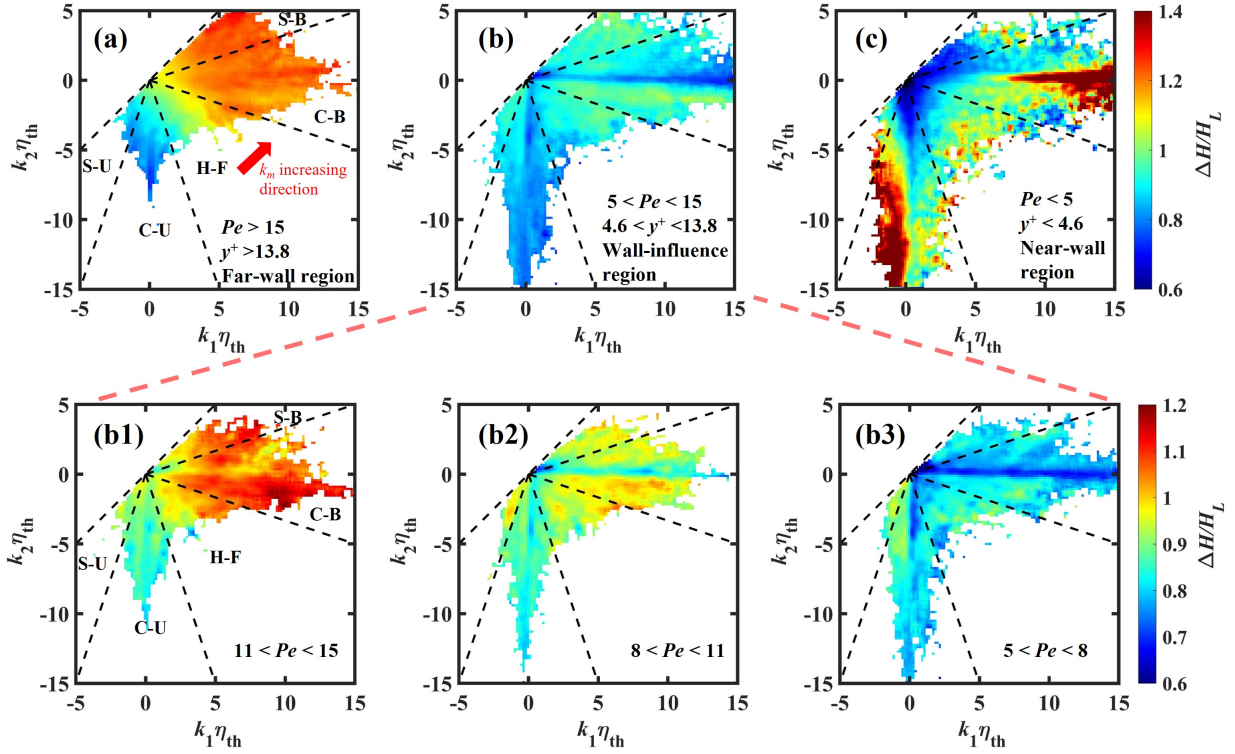


Figure 8. Mean values of heat release rate conditioned on (k_1, k_2) in different near-wall turbulent regions.

high levels of $\Delta H/H_L$ are mainly concentrated in parts of the C-U and C-B regions as observed in Fig. 7(c). Near the region where k_m approaches 0, there is a noticeable decrease in HRR. Obviously, that analyzing flame $\Delta H/H_L$ characteristics under different three-dimensional structures based on flame principal curvature can further reveal the relationship between flame reaction intensity and flame surface geometric structure. Additionally, in the near-wall region, the mutual relationship between $\Delta H/H_L$ and flame surface geometric features exhibits a higher degree of complexity, indicating that relying solely on k_m to study the geometric characteristics of near-wall flames may not be sufficient.

CONCLUSIONS

In the current study, a three-dimensional direct numerical simulation (DNS) was conducted, considering the premixed H_2 -air flame in turbulent channel flow. The near-wall flame's

fractal geometry has been investigated by evaluating its local principal curvatures and principal tangent vectors. Based on that, the effect of the flame-wall geometric relationship on the near-wall flame quenching characteristics is further discussed with the near-wall flame's heat release rate (HRR). The findings are as follows:

As the flame approaches the wall, there is a significant development in its topological features, with the cylindrical shaped flame takes the dominance in the near-wall area, convex towards the burned or unburned gas.

The cylindrical flame mostly exists in the near-wall area aligned primarily with the wall parallel direction.

There is a positive correlation between the flame's HRR and mean curvature in the far-wall area. But this correlation diminishes in the near-wall area with a significant decrease of HRR for the flame convex to the burned gas.

Compared with that of far-wall area, there is a greater level of complexity in the correlation between the HRR and

flame's geometric features in the near-wall area, which can be more accurately represented by the flame's principal curvatures than by the mean curvature alone.

REFERENCES

- Bradley, D., Gaskell, P. H. & Gu, X. J. 1998 The modeling of aerodynamic strain rate and flame curvature effects in premixed turbulent combustion. *Symposium (International) on Combustion* **27** (1), 849–856.
- Chakraborty, Nilanjan & Cant, Stewart 2004 Unsteady effects of strain rate and curvature on turbulent premixed flames in an inflow-outflow configuration. *Combustion and Flame* **137** (1-2), 129–147.
- Chakraborty, Nilanjan & Klein, Markus 2009 Effects of global flame curvature on surface density function transport in turbulent premixed flame kernels in the thin reaction zones regime. *Proceedings of the Combustion Institute* **32 I** (1), 1435–1443.
- Echekki, Tarek & Chen, Jacqueline H. 1996 Unsteady strain rate and curvature effects in turbulent premixed methane-air flames. *Combustion and Flame* **106** (1-2), 184–190.
- Gashi, Sara, Hult, Johan, Jenkins, Karl W., Chakraborty, Nilanjan, Cant, Stewart & Kaminski, Clemens F. 2005 Curvature and wrinkling of premixed flame kernels-comparisons of OH PLIF and DNS data. *Proceedings of the Combustion Institute* **30** (1), 809–817.
- Gruber, A, Sankaran, R, Hawkes, E R & Chen, J H 2010 Turbulent flame-wall interaction: A direct numerical simulation study. *Journal of Fluid Mechanics* **658**, 5–32.
- Göktolga, M. Uğur, de Goey, L. Philip H. & van Oijen, Jeroen A. 2021 Modeling curvature effects in turbulent autoigniting non-premixed flames using tabulated chemistry. *Proceedings of the Combustion Institute* **38** (2), 2741–2748.
- Kaddar, Driss, Steinhausen, Matthias, Zirwes, Thorsten, Bockhorn, Henning, Hasse, Christian & Ferraro, Federica 2023 Combined effects of heat loss and curvature on turbulent flame-wall interaction in a premixed dimethyl ether/air flame. *Proceedings of the Combustion Institute* **39** (2), 2199–2208.
- Kosaka, Hidemasa, Zentgraf, Florian, Scholtissek, Arne, Hasse, Christian & Dreizler, Andreas 2020 Effect of Flame-Wall Interaction on Local Heat Release of Methane and DME Combustion in a Side-Wall Quenching Geometry. *Flow, Turbulence and Combustion* **104** (4), 1029–1046.
- Li, Juan, Zhao, Zhenwei, Kazakov, Andrei & Dryer, Frederick L. 2004 An updated comprehensive kinetic model of hydrogen combustion. *International Journal of Chemical Kinetics* **36** (10), 566–575.
- Poinsot, T J, Haworth, D C & Bruneaux, G 1993 Direct simulation and modeling of flame-wall interaction for premixed turbulent combustion. *Combustion and Flame* **95** (1-2), 118–132.
- Tanahashi, Mamoru, Fujimura, Masanobu & Miyauchi, Toshio 2000 Coherent fine-scale eddies in turbulent premixed flames. *Proceedings of the Combustion Institute* **28** (1), 529–535.
- Wang, Peiyong, Hu, Shengteng & Pitz, Robert W. 2007 Numerical investigation of the curvature effects on diffusion flames. *Proceedings of the Combustion Institute* **31 I** (1), 989–996.
- Xuan, Yuan, Blanquart, Guillaume & Mueller, Michael E. 2014 Modeling curvature effects in diffusion flames using a laminar flamelet model. *Combustion and Flame* **161** (5), 1294–1309.
- Zhang, Feichi, Zirwes, Thorsten, Häber, Thomas, Bockhorn, Henning, Trimis, Dimosthenis & Suntz, Rainer 2021 Near Wall Dynamics of Premixed Flames. *Proceedings of the Combustion Institute* **38** (2), 1955–1964.
- Zhao, Peipei, Wang, Lipo & Chakraborty, Nilanjan 2018 Analysis of the flame-wall interaction in premixed turbulent combustion. *Journal of Fluid Mechanics* **848** (June), 193–218.